Terrestrial Planet Finder Cryogenic Delay Line Development

Robert F. Smythe*, Mark R. Swain, Oscar Alvarez-Salazar, James D. Moore
Jet Propulsion Laboratory 4800 Oak Grove Drive, Pasadena, CA, USA, 91109

ABSTRACT

Delay lines provide the path-length compensation that makes the measurement of interference fringes possible. When used for nulling interferometry, the delay line must control path-lengths so that the null is stable and controlled throughout the measurement. We report on a low noise, low disturbance, and high bandwidth optical delay line capable of meeting the TPF interferometer optical path length control requirements at cryogenic temperatures.

Keywords: nulling, interferometer, cryogenic, path-length.

1. Introduction

The Terrestrial Planet Finder (TPF) interferometry mission would require the co-phasing of light from four different telescopes to sub-nanometer precision. This goal would be accomplished by the use of an optical path-length controlling delay line. The dynamic range requirements would have to be scaled to the positioning stability that could be achieved by a formation of four free-flying telescopes and a fifth beam combiner spacecraft. Getting a the long period of observation necessary to measure deep nulls requires high bandwidth disturbance rejection, and meeting the mission goals in sensitivity, every part of the optical beam path would have to be cooled to less than 40 degrees Kelvin[1]. To date, very little work has been done to explore the technology required to meet these constraints. Our experiment attempted to meet these requirements using a two-stage mechanism under servo control. There is a wealth of experience operating optical delay lines of this type in our group that was exploited for our purposes, particularly from research done for the Keck Interferometer (KI) and Space Interferometry Mission (SIM). Our initial performance expectations of our prototype delay line design inherited directly from KI.

2. Performance goals

In the absence of more clearly defined requirements at the beginning of the experiment, we set our own performance goals keeping the prototypical character of the stage, and the TPF Technology Plan in mind.

- Optical Path Delay (OPD) ~0.2m = 0.1m physical travel
- Static path length control: 20nm RMS
- Closed-loop bandwidth: 100 Hz
- Open-Loop slew velocity: ~0.01 m/sec
- Operation Temperature: 77 ^{o}K

To this list of performance targets we added a velocity-tracking goal of 20nm RMS @ 100μm/sec for greater than 30 seconds. We knew from the outset that the RMS error required for TPF nulling was more likely to be 4-5nm, but a large part of our agenda was to decide whether a 2-stage servo would be adequate to achieve this level of path length control, an optimistic goal with an untried prototype. During the year, deeper analysis of the error terms in the budget tightened this specification to 0.2nm.

* Send correspondence to: rsmythe@huey.jpl.nasa.gov; (818) 354-5926, fax (818) 393-4357; m/s 171-113, 4800 Oak Grove Drive, Pasadena, CA 91109

3. Delay line description

Our delay line has a 2-stage design for Z-axis control, the outer stage is moved by a stepper motor for coarse stage positioning, the inner stage is driven by a long throw Piezo-electric transducer. The inner stage carries a 0.5" retro-reflecting corner cube to return the metrology. In this configuration there is no other optics on the delay line. The Optical Path Delay (OPD) command to the delay line measures from the metrology beam-splitter to this corner cube.

3.1 The coarse stage

The coarse stepper driven stage resembles a porch glider (see Fig. 1 next page). It is flexure-based providing stiffness and good positioning repeatability, as well as orientation independence. We measured the tip-tilt errors of the coarse stage at the ±2 arcsecond level[2]. The errors follow a repeatable profile that depends upon stage position, so compensating for these errors could be accomplished by simple means. Depending on the material used, and the angle operated over, the flexures could be expected to last through a nearly infinite number of cycles. It also has the potential to offer a long range of travel, up to 10cm in the current configuration. It is actuated by a band drive system based on straps. The action of the straps upon the stage is indicated by the arrows. The inner stage pulley is linked to the outer stage pulley by an "S" shaped strap, so their motion is coupled. In order to keep the inner stage moving in a straight line, thereby removing optical shear, the ratio of movement of inner to outer stages is 2:1. Hence the pulleys that drive the respective stages have radii in a ratio 2:1. Springs are used to provide tension against the drive straps, coil springs for the outer stage and a constant force spring for the lower stage. Our first design iteration had coil springs on the lower stage but this created a position dependant resonance that moved between 60Hz and 80Hz. It was undesirable to add a wide gain peak to suppress such a broad band of frequencies in the control law, so the constant force spring was a good solution for this. The coil springs for the outer stage did not have much tension, so did not strongly influence the PSD. We performed a "modal hammer" accelerometer characterization of the un-actuated structure, but the modes identified in this test did not give us much trouble, probably because of the slow rates at which we drove the stage.

The choice of stepper motor evolved through the course of the year as we got an initial assessment of the stage performance. Initially we were using a 200step/rev motor with a driver module also, with a 20microstep/step positioning resolution. From our initial characterization of the stage using this combination, it quickly became apparent that the impulse energy of these large steps was exciting a moving 60Hz-80Hz resonance (depending on stage position) in the stage that would have been impossible to control. To solve this we attempted to damp the structure in a number of different ways: lead shot, a flexure coupling between the motor and stage, and friction applied to the drive straps and preload springs. We also attempted to put a gain peak in the center of the range at 70Hz. None of these methods solved the problem completely, or in a way that we believed would function at cryogenic temperatures. We finally changed to a Parker Zeta4™ stepper motor drive, one that applied smaller micro-steps (254microsteps/step), and had a form of electronic damping that smoothed the impulse injected into the structure. We also switched from a 200step/rev to a 500step/rev motor, further reducing the individual step size. The final working resolution of the stepper motor stage is 15 nanometers per micro-step. This is probably finer resolution than is absolutely necessary given the overlap with the delay range of the PZT, but did quiet the slew of the structure down considerably.

The ordering literature from the stepper motor manufacturer did not illuminate the torque differences between the 500step/rev motor and the 200step/rev motor, but that effect was about -15%. There is also a ~10% drop in torque when you operate the motor in a microstep mode, as well as an additional (undocumented) 10% torque reduction between the stepper motors built for open air, room temperature operation and vacuum/cryogenic operation. To compensate for these accumulated effects, typically we would reduce the stepper motor phase current for warm operation, and increase it to the rated current for cryogenic operation. Unfortunately we learned of the torque differences the hard way, by cooling down the experiment and being unable to move the stage.

Because of the long lead times associated with ordering a cryogenic/vacuum rated motor with a sufficient torque margin, we came up with two different schemes for using an under-powered motor with a 5:1 reducer in order to maintain our project schedule. In order to be assured of some path to successful closed-loop operation of the delay line, we put into motion three different strategies, all initiated in parallel. Two of them involved variants of the 5:1 reducer mentioned before.

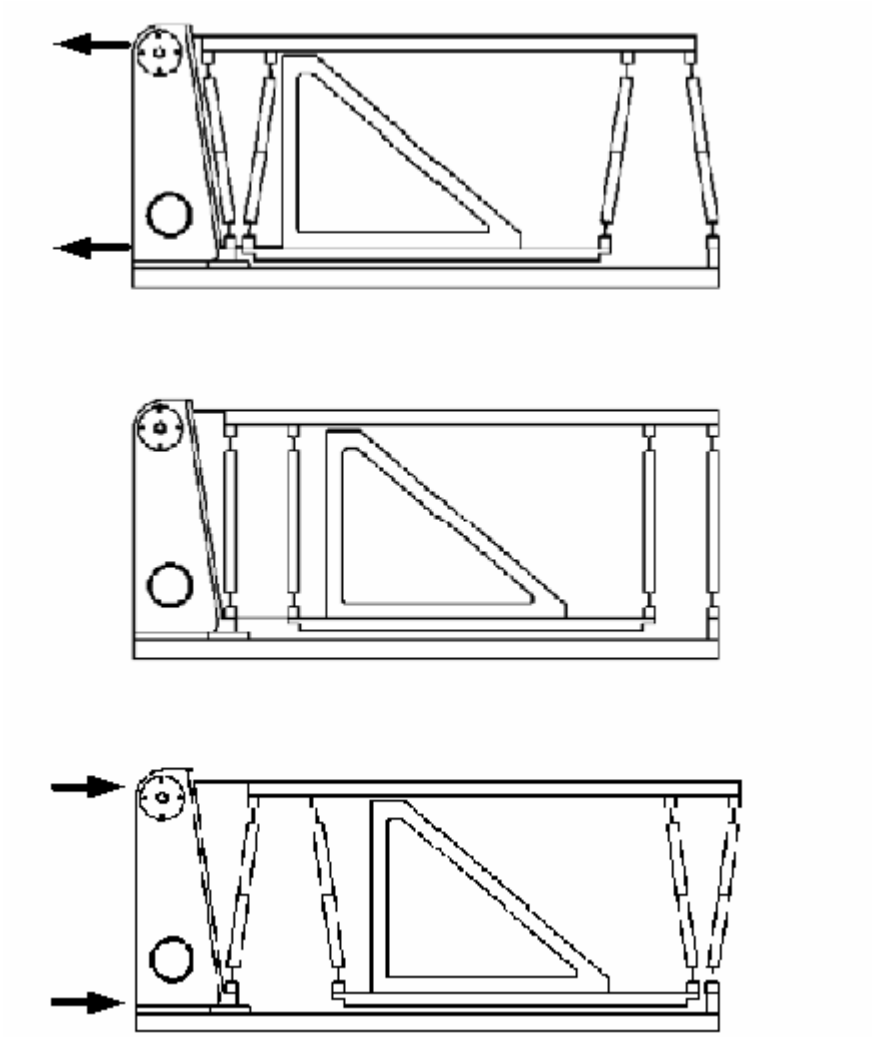

Fig. 1. Delay line coarse stage action

The third approach was to purchase a new stepper motor, possessing a healthy torque margin to be delivered after our scheduled project completion. This was to be our ace in the hole, in the event that both the reducers failed to properly move the coarse stage. The first reducer was comprised of a pair of pulleys, with the radial in a ratio of 5:1, the smaller pulley mounted on the output staff of the motor. The larger pulley was mounted coaxially with the lower stage pulley. The pulleys were connected by a stainless steel constant force spring. The spring was bolted to large pulley and bonded to the smaller pulley. Although this worked admirably at room temperature, during the cool down cycle, the bond joint to the smaller pulley failed. Fortunately, by this time the part set for the second reducer had been manufactured and acquired. This reducer was a custom made (matched CTE) stainless steel gearhead. This had square cut gears so we expected that it would have a "rumble" that would drive up the RMS error. We measured this increase in velocity tracking error at 12nm RMS. When we sampled metrology while moving the stage, the PSD showed the addition of a velocity-dependant set of harmonics that did not appear with any other drive means. As we were rapidly running out of time, we decided to make an attempt to collect tracking data with this gear reducer, as we had not yet successfully moved the coarse stage cold.

The expensive motor also has a correspondingly higher quality gear head, and velocity dependant harmonics are absent if not substantially reduced, with an expected reduction in the overall RMS error. With a comparable room temperature motor we saw a best ever 14nm RMS error while tracking a 100μm/second velocity target.

3.2 The fine stage

The fine positioning control of the delay line is controlled by a single Piezoelectric Transducer (PZT), driving a momentum-compensated mechanical amplifier. The mechanical amplifier resembles an elongated parallelogram with pairs of flexures along each side. The PZT is compressed along the axis of the long diagonal of the parallelogram by support flexures at each end. The expansion of the PZT along the long diagonal causes the ends of the short diagonal to move toward each other with a motion amplified by a factor of three or four.[3]

Based on the following assumptions:

- 90μ total throw at 77K
- 16-bit DAC

The minimum resolution of the PZT stage is 6nm cold. This is corroborated by an amplitude transfer function plot shown below without our default operational integrating output, where for each PZT count input, there is an output of 11 laser counts. One laser metrology count is equal to 633nm/1024 or 0.62nm.

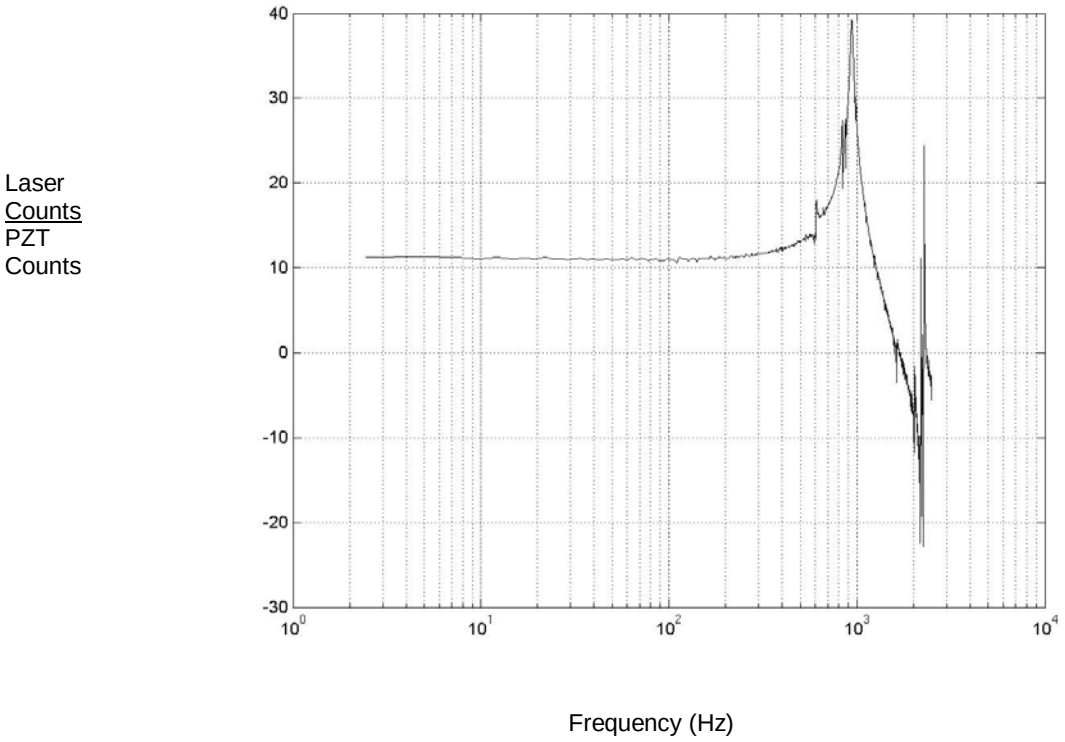

Fig. 2. Amplitude Transfer function of PZT Stage at 80K

The data was taken by injecting a Gaussian, random signal into the PZT amplifier, synched to an output metrology measurement. The metrology sample rate was 5 KHz. The manufacturer quotes the natural unloaded resonant frequency of the bare PZT as 9 KHz. Of course any mechanical mounting at all would drop this number considerably. The prominent resonance at 940Hz is probably due to the mechanical amplifier. Reflecting upon the resolution of the stepper motor stage, we could have benefited from a shorter throw actuator with finer resolution. Our PZT driver board provided a convenient location to low-pass filter the output, removing any high frequency noise coupled in by our stepper motor drive, but this was not attempted.

3.3 Facilities

At the beginning of the experiment we were not operating in a lab space that permitted the use of a large volume of cryogens, nor could it have fit the large Dewar and lifting device needed to open it. In November of 2002 we moved to a more suitable location that had an exterior wall for our nitrogen vent. We set up the delay line and metrology on a

Newport 4’ X 8’ table with pneumatic air isolating legs. When this was done it was quickly apparent that there was inadequate overhead clearance to lift the 30” bell of the dewar above the height of the nitrogen fill pipe. The crane was also helpful, if not necessary, to lift the internal radiation shield (60lbs). To alleviate this we had to both shorten the table isolation leg length and modify the lifting fixture to extend its height to the point where it was in contact with the tiles of the suspended ceiling when unloaded. Great care was taken while moving the bell to avoid shearing off the sprinkler heads.

Pfieffer Vacuum™ made the Turbo-molecular pump station. It is mentioned in this report because we had some trouble with it, the recounting of which may save some time for others. Initially, to save money the backing stage of the two-stage pump was under specified for the volume of the chamber, requiring at least five hours of roughing before the turbo could be turned on. In general the maximum pressure level where we would have added the pumping action of the turbo stage was ~60mbar. In February, after only a few pump-down cycles the turbo section failed. The vendor was very helpful and sent a replacement unit very rapidly, which we retrofitted ourselves to save time. At the same time we installed an higher volume backing pump, further reducing our pump-down time. The pump-down time (from atmospheric pressure to ~10e-4 mbar) went from ~72 hours to ~36 hours. Once this pressure was reached, we could start adding cryogens. The elapsed time from the first addition of cryogens to the attainment of a sufficiently low operating temperature was approximately 30 hours. We developed a system for using dry nitrogen to force the liquid nitrogen out of the 50-liter vessel in a short time, after which it was safe to vent the Dewar and remove the bell to perform a repair or modification to the delay line. We made no effort to avoid thermal shock to the contents of the Dewar.

The Dewar was designed and built for ~$50K by Precision Cryogenics™ with 10 KF-40 flanges for electronic feed-through, one large 10” opening to provide space for 3” stacked optical paths, and one ISO-63 flange opposite the optical opening for a potential beam re-routing option. The top of the 50 liter liquid nitrogen vessel is formed by a thick circular aluminum plate, with ¼-20 tapped holes on a 2” grid, about 40” across. There are three optical paths into the Dewar, two of which are superfluous in our current configuration. These are the 3.5” furnace glass windows that could carry a stacked pair of 3” beams but at present just give us a look at the delay line. The openings are large enough to let us look around the back at the stepper motor assembly by use of a judiciously placed fold mirror. The only “real” optical element other than the metrology returning corner cube is the 1.5” anti-reflection coated window to pass the HeNe metrology beam. It not wedged but set in its mount at an angle to prevent back reflection.

Fig. 8. The crane and radiation shield, optical table with delay line, and Dewar bell

4. Software tools and control system design

4.1 Software tools

The metrology system used in this experiment was the Zygo™ ZMI2002, a VME based system that required the creation of a software driver. This was performed in 2 stages: a first vxWorks™ driver written in C to read the contents of the 36bit position register to a file in a fast loop, up to 5KHz; a second driver was written in C++ that performed the same task but interfacing to the Real Time Control toolbox (RTC) framework. This software environment is a JPL product for hard real-time control of distributed systems and is used in other interferometry projects, notably for the KI, SIM, and Micro-Arc-second Metrology (MAM) projects. The delay line software was a reduced form of the 3-stage KI delay line. This made it easy to recycle developed software for the JPL produced PZT and stepper motor controller board and the synchronizing RTC Timing board. The coarse stage (stepper motor) followed the commanded velocity target in a predominantly open-loop fashion, and the residual error between the target and the actual stage position was minimized by the PZT operating closed loop. The closed loop portion of the stepper motor operation involves using a proportional, integral, derivative (PID) filter (just P in our case) to desaturate the PZT. In other regards RTC configuration and telemetry had all the built in facility to construct and tune the servo for PZT, derive transfer function information, gather background vibration data, provide target modulation, and tune the ratio of stepper-motor steps to laser counts.

The logistical complication of operating a large cryogenic vacuum Dewar made it desirable to remotely monitor the temperature and pressure of the vessel through the RS232 ports provided on those sensors. We were able to take advantage of resources developed for KI and MAM to fill these needs. Good pressure and temperature information was critical to the project in shortening the Dewar cycle times, often the governing factor in development.

4.2 Control System

As mentioned previously, the RTC software package included all the tools needed for characterization, implementation and tuning of the two-stage servo system. The real-time code was running on a Motorola™ MVME2304-0133 single board processor. The PZT Motor board had an optional integrating output for the PZT drive, which was preferred over the pure DAC for its smoother response. Therefore, by default, the measured PZT stage open-loop response has a slope of $1/f$. Figure 3 is a plot of the measured transmissibility from disturbance to OPD at the PZT stage. This figure clearly shows the 1/S feature mentioned above in addition to two stage flexible modes at 600Hz and 940Hz. Warm and cold measurements are shown. In addition, the bode-plot of the cold transmissibility function model is shown in Figure 3. This model was used in the design of the control laws, which were ultimately implemented in the servo system.

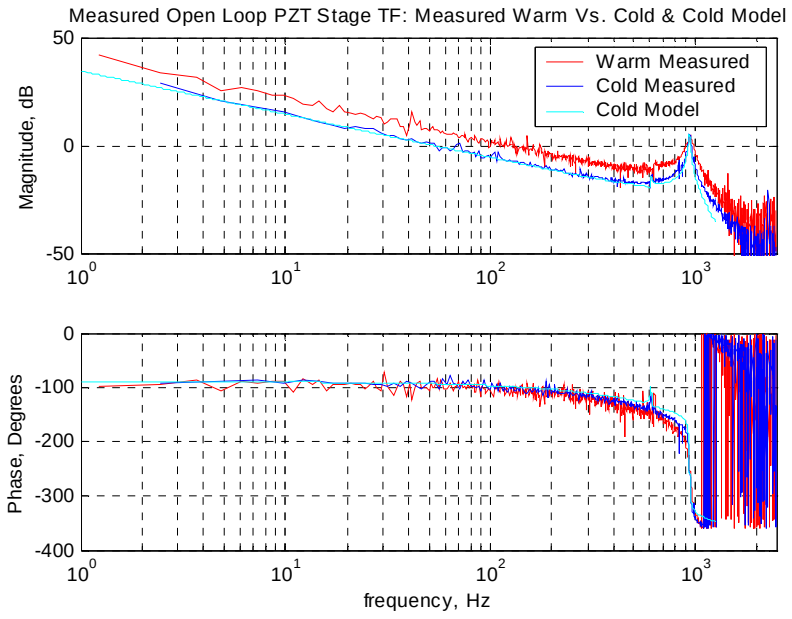

Fig.3. Open loop plant transfer function and model

The control law design strived to have nearly infinite gain at DC and as much gain as possible below 100Hz, which is where most of the OPD energy is found: 2.8μm from DC to 100Hz, and 0.020μm above 100Hz. Limited by the real time system's sampling rate and processing speed, the bandwidth of the closed loop servo system was expected to be below 500Hz. In fact, 300Hz closed loop bandwidth was achieved in the presence of the 600Hz flexible mode (i.e., the energy in this mode reduced our gain margin and directly limited our bandwidth). The control law was designed to have a slope of $1/f^2$ below 300Hz, and uses some phase compensation to increase

the tracking fidelity within this band, and implements a narrow notch filter at 940Hz to minimize lag issues and avoid feeding back energy from this mode. System noise is low, and since the bandwidth was limited by the 600Hz mode, no efforts were made to implement an optimal stochastic controller. The loop shape obtained for the servo system is shown in Figure 4. The loop shape shown in this figure is the output of our control system design script. Measurement of this quantity is not possible because the high DC gain feature in the control law saturates the PZT servo stage when the loop is not actually closed. Note that the phase margin is about 30°, and the gain margin is about 10dB. As stated before, the delay line servo was augmented by a desaturation stage that makes use of the stepper motor stage to keep the PZT near its mid range.

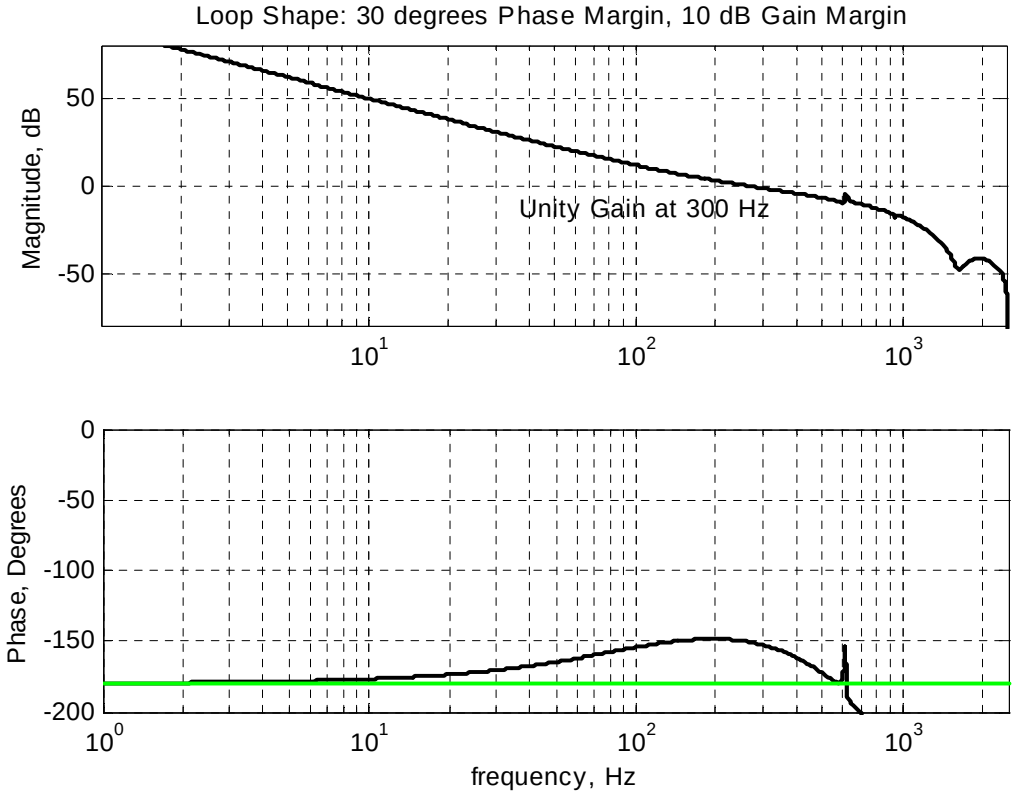

Fig. 4. Simulated Loop Shape

In Figures 5 and 6 on the next page we show a comparison of measured "cold" performance and a prediction of performance using the filtering method. This method has to be used given that we don't have access to the actual system's disturbance. Given the lack of modal density in the low frequencies, this method of predicting the closed loop performance is adequate as shown in the Figures. Note that in Fig. 6, below 10Hz the predicted and measured performances are both below 3.5nm RMS. The cumulative measured performance below 300Hz is 31.5nm RMS, whereas the cumulative predicted performance below 300Hz is 34nm RMS. Given that this system's OPD is a random process; our prediction of closed loop performance is arguably adequate for control law design. It is worth mentioning here that our system model corresponds to a low velocity time invariant motor stage. A more complete non-linear motor model would allow for a more complete set of analysis and control law designs for a wider range of operating regimes, which are out of scope of our experiment. We did not, for example, attempt to characterize closed loop tracking at a wide variety of rates. As you might expect, we found that trying to track faster than our goal of 100μm/sec increased our RMS residual, tracking slower made the residual smaller.

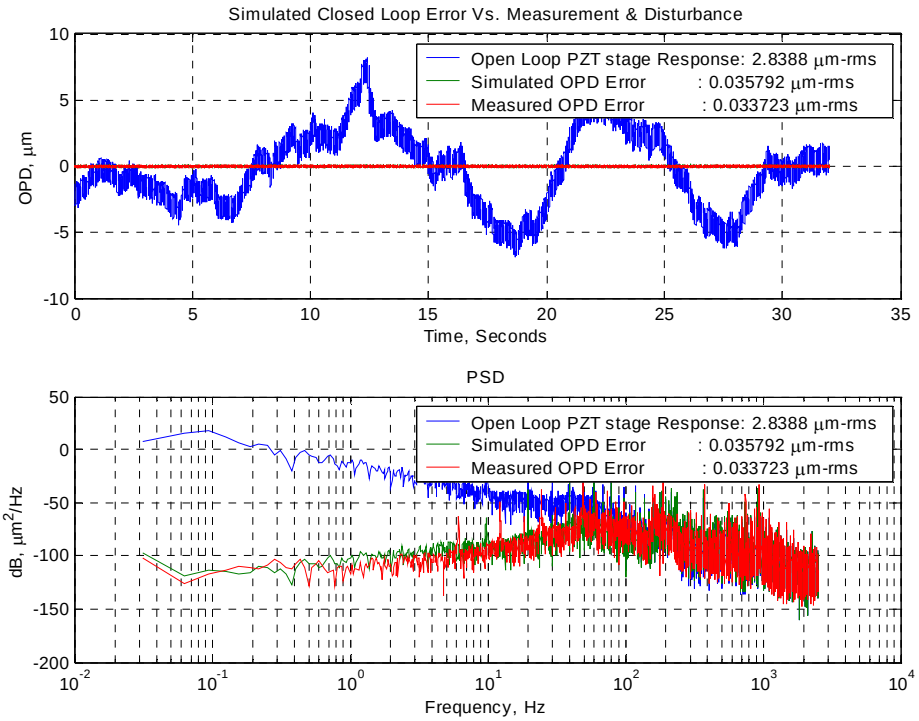

Fig. 5. Measured OPD, Open & Closed Loop Vs. Simulated Closed Loop, PSD

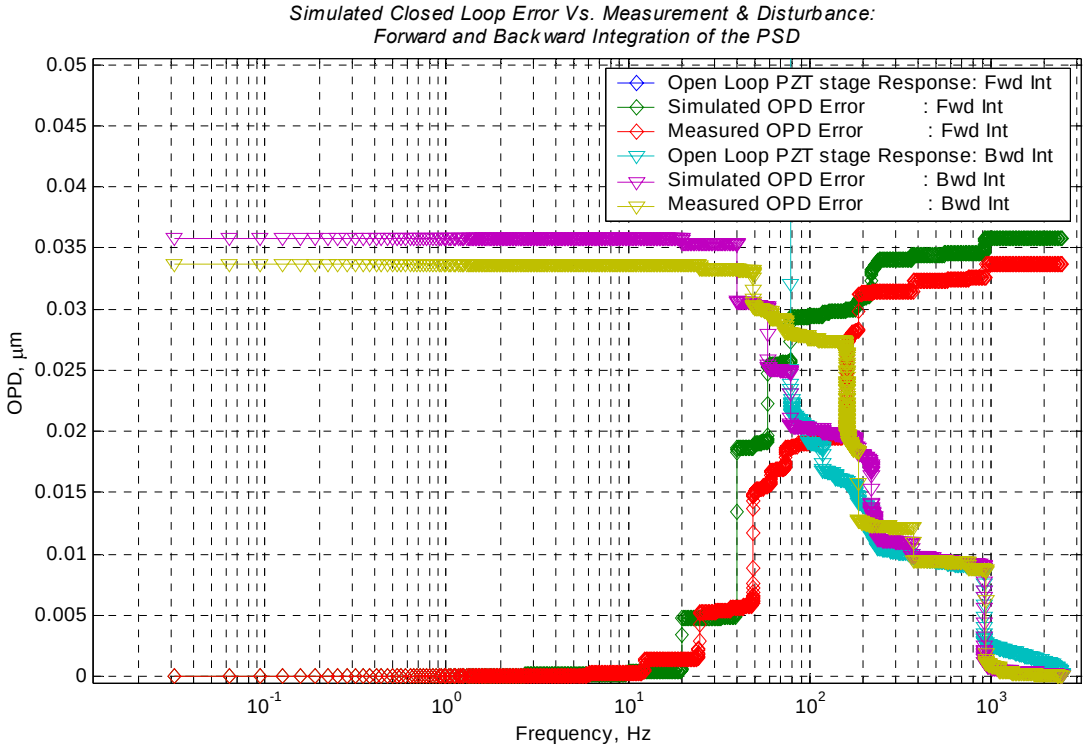

Fig. 6. Measured OPD, Closed Loop Vs. Simulated Closed Loop: Integrated PSD

5. Performance Results

Below is a table summarizing our performance targets. It does encapsulate data from the plots and discussion on previous pages.

Performance	**Target**	**Achieved**
Optical Path Delay (OPD)	0.2m	0.1m
Static path length control	20nm RMS	11.4nm RMS
Closed-loop bandwidth	100Hz	300Hz
Open-Loop slew velocity	1cm/sec	0.25cm/sec
Operation Temperature	77 ºK	88 ºK
Dynamic path length control @ 0.1mm/sec	20nm RMS	28.8nm RMS

Table 1: Performance goals and results

6. Discussion

The OPD goal was not met primarily because of the small torque margin of the motor; while in our warm checkout routine prior to closing up the Dewar, we found that we could pull the stage through most of its travel, but when operated near the back of travel, the motor would stall and the stage would slip toward the front under the tension of the constant force return spring. A certain minimum force was required to keep adequate tension on the inner and outer drive bands, below which the stages did not drive in parallel. At the front of the travel there was a short region where there was inadequate tension and the inner and outer stage would bind together. In the absence of a motor with an adequate torque margin we had no choice but to limit the stage travel with limit switches to stay out of these trouble spots, resulting in a net stage travel of only 5cm. Another casualty of the under-specified motor was the open-loop slew target. All our measurements of this were taken by commanding a motor velocity from a dead stop. It is probable that we could have done better by modifying the software to perform a "move-to" action that would have permitted a typical trapezoidal accelerate/steady-state/decelerate profile. We did not feel that the time to achieve this would be well spent because simply using a stronger motor would do more to improve the delay line. The last place the motor torque let us down was in the dynamic path length control. We know that with an adequate torque margin the 5:1 supplemental gearhead would not have been needed. With a motor designed for an STP environment, and more torque margin, we saw a best performance of 14.2nm RMS at 0.1mm/sec. We inferred that if our existing motor, with the supplemental gearhead, went from 22nm to 28nm cold, that most of the increase was due to loss of mechanical gain of the PZT in the cryogenic environment. Following that reason, we could anticipate that with the right motor, and a high precision gearhead, we would have a 6nm increase in the RMS error and barely make the 20nm target. Another contributor to this error that must be accounted for is the out-of-band 940Hz broad resonance. It is possible that we would still have adequate dynamic range of the PZT stage without the mechanical amplifier, and the resonance might be absent, or less broad. We can see both in the open loop transfer function in figure 3 and the integrated PSD in figure 5 that 940Hz is a significant contributor to the RMS error.

The 88°K delivered for the cryogenic operating temperature was measured at the PZT mechanical amplifier, the closest point to the optical path. The mechanism is connected to the cold plate only by the stage flexures, and is unable to keep up with the thermal loading of the PZT leads. Simultaneously, we measured 78°K at the cold plate, 85°K at the inner stage (connected to the cold plate thru the same flexures as the PZT, but with only the temperature sensor wires thermal loading), and 94°K at the stepper motor. This could have been improved by using a copper thermal strap. In Figure 9 on the next page we show one day worth of temperature data logging. Between 01:00GMT and 02:30GMT we were operating the stepper motor and PZT in nearly continuous tracking of a 0.1mm/sec triangle wave target. In that time the stepper motor increased in temperature by 31°K, or about 0.34°K/min. The two-phase motor had a measured impedance of 1.3Ω, and was drawing 1.24A/Phase for a thermal load of 2watts. The top trace is that of the stepper motor, below that is the PZT mechanical amplifier, below that is the inner stage of the delay line carrying the PZT. The bottom trace is the

cold plate. Only the two center traces are taken with sensors near the optical beam path, so our design would effectively keep superfluous emmissivity out of the science beam.

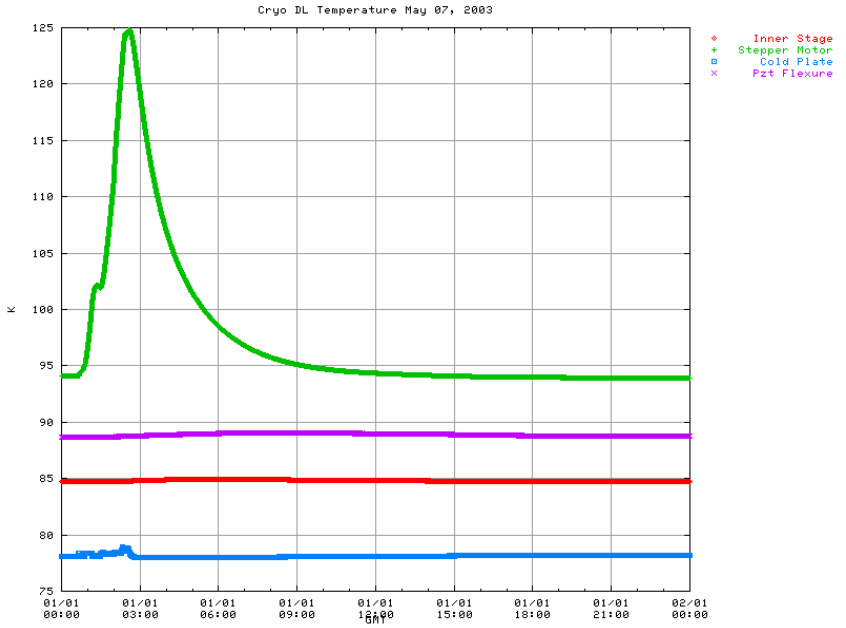

Fig. 9. Temperature data logging 5/07/03

7. Future work

We can suggest several improvements to the delay line. The first and most obvious is installing the higher torque stepper motor. This would reduce the amount of error due to the 5:1 gear reducer we applied. It would also improve the open loop slew speed and, by virtue of the stronger strap tensioning springs, lengthen the amount of available OPD. This however might be less effective overall than performing a complete redesign of the stage. One of the things we noticed early on in the stage characterization is that the stage lacked any loss mechanism to provide damping, other than that inherent in the metal of the flexures. It would be useful to explore methods to achieve this, and an eddy current damper comes to mind. Making an effort to more closely match the overlap of dynamic range of the coarse and fine stages would probably drive the OPD errors down further. It is likely that a PZT stage with only 30μm (cold) would be sufficient to suppress the stepper motor residual, and also give a theoretical control resolution of 2nm/PZT count. One thing to remember about this stage is that we are not moving anything other than a 0.5" corner cube at high bandwidth, no large parabolic mirror is being moved by the stepper stage for a cats eye configuration. This would obviously increase the mass here, but the focus mirror associated would be small and could be moved as fast as the corner cube. Our group currently favors a roof-top mirror however, and these would of necessity be heavier and more difficult to move at high bandwidth, and in a momentum compensated way. One of the metrics missing from our performance targets is that of tip-tilt and/or beam shear, depending on the optical layout chosen. The delay line will have its own tip-tilt compensation. This is envisioned to be a low bandwidth task

At the beginning of the year it was of great interest to us to find out if the whole job of OPD control from centimeters to nanometer levels would be possible with only two stages. The RMS error specification from the TPF project has been reduced by an order of magnitude in the last year and it is evident now that a third, high bandwidth, high-precision stage is now needed. The right actuator is not now available commercially, but what we envision is a very short throw (1-5μm), single axis PZT, using metrology data clocked directly from the VME bus at tens to hundreds of kilohertz (the Zygo laser metrology gauge 2002 supports up to 3MHz external sampling) and processing the eight least significant bits of data with high speed A/D to feed an error signal to either an analog controller or a high speed digital signal processor.

Acknowledgements

The work described in this publication was carried out at the Jet Propulsion Laboratory, California Institute of Technology, under a contract with the National Aeronautics and Space Administration. We would like to thank the following individuals for their contribution to the project: Phillip Dumont[a], Michelle Creech-Eakman[b], Jean Garcia[a], Marco Hernandez[a], Erik Hovland[a], Rich Johnson[a], and Jason Shupe[a.]
[a] Jet Propulsion Laboratory, 4800 Oak Grove Drive, Pasadena, CA, USA 91109
[b] Dept. of Physics, New Mexico Institute of Mining and Technology, 801 Leroy Place, Socorro, NM, USA 87801-4796

References

[1] C. A. Lindensmith ed., "Technology Plan for the Terrestrial Planet Finder," JPL Publication 03-007, Rev B, March 7, 2003

[2] M.R. Swain, P.J. Dumont, P.R. Lawson, J.D. Moore, R.F. Smythe, C.K. Walker, and C.Y. Drouet d'Aubigny "Far-infrared interferometer technology development: a progress report," SPIE Conf. 4852, *Interferometry in Space*, M. Shao ed., 465-651 (2003), 22-28 August 2002, Waikoloa, HI.

[3] R. Calvet, P. Lawson, J. Moore, M. Swain, "Mechanical Amplifier for a Piezoelectric Transducer," NASA Tech Briefs, February 2003, Vol.27, No.3